Predictive control of multizone heating, ventilation and air-conditioning systems in non-residential buildings

Antoine Garnier, Julien Eynard, Matthieu Caussanel, Stéphane Grieu

Predictive control of multizone heating, ventilation and air-conditioning systems in non-residential buildings

Antoine Garnier[a,b], **Julien Eynard**[b,c], **Matthieu Caussanel**[b,c], **Stéphane Grieu**[b,c,*]

[a] *Pyrescom, Mas des Tilleuls, 66680 Canohès, France*
[b] *PROMES-CNRS, Rambla de la Thermodynamique, Tecnosud, 66100 Perpignan, France*
[c] *University of Perpignan Via Domitia, 52 Avenue Paul Alduy, 66860 Perpignan, France*

Abstract

In France, buildings account for a large part of the energy consumption and carbon emissions. Both are mainly due to Heating, Ventilation and Air-Conditioning (HVAC) systems. Because older, oversized or poorly maintained systems may be using more energy and costing more to operate than necessary, new management approaches are needed. In addition, energy efficiency can be improved in central heating and cooling systems by introducing zoned operation. So, the present work deals with the predictive control of multizone HVAC systems in non-residential buildings. First, a real non-residential building located in Perpignan (south of France) has been modelled using the EnergyPlus software. We used the Predicted Mean Vote (PMV) index as a thermal comfort indicator and developed low-order ANN-based models to be used as controller's internal models. A genetic algorithm allowed the optimization problem to be solved. Using the proposed strategy, the operation of all the HVAC subsystems is optimized by computing the right time to turn them on and off, in both heating and cooling modes. Energy consumption is minimized and thermal comfort requirements are met. In order to appraise the proposed management strategy, it has been compared to basic scheduling techniques. The simulation results highlight the pertinence of a predicitive approach for multizone HVAC systems management.

Keywords: multizone heating, ventilation and air-conditioning system, non-residential building, predicted mean vote, predictive control, scheduling technique, feedforward neural networks, cascade correlation algorithm, genetic algorithm.

1. Introduction

Within non-residential buildings, almost half of the energy consumption is due to Heating, Ventilation and Air-Conditioning (HVAC) systems [1]. In addition, older, oversized or poorly maintained systems may be using more energy and costing more to operate than necessary. As a consequence, new approaches dealing with energy ressources management are needed to make HVAC systems more efficient. First, energy efficiency can be improved in central heating and cooling systems by introducing zoned operation. This allows a more granular application of heat and each HVAC subsystem can be controlled independently. Another key point is thermal comfort. Thermal comfort can be defined as "that condition of mind which expresses satisfaction with the thermal environment" [2]. It is mainly related to indoor conditions and impacted by both the effectiveness of the building envelope and the way the HVAC system is used.

Many research studies focusing on improving the operation of centralized or zoned HVAC systems have been conducted over the last few years. Recently, Haniff et al. provided a detailed review of basic, conventional, and advanced HVAC scheduling techniques [3]. First, the "interruption", "Early Switch-Off" (ESO), "Pre-heating (or pre-cooling) in the Demand Reduction" (DR), and "Alternate Switch-On/Off" (ASOO) basic scheduling techniques are discussed. The "interruption" technique consists in suspending the HVAC operation for several hours during occupancy periods. In opposition, in case of the ESO technique being used, the HVAC system is (usually) stopped two hours before people leave the building. The DR technique is about pre-heating (or pre-cooling) a building during off-peak periods (i.e. non-occupancy periods). Finally, the ASOO technique is based on alternately switching on and off the HVAC system during office hours [4].

Usually, with a conventional scheduling technique, the HVAC system operates 24 hours a day and the "night setback" mode allows energy saving objectives to be achieved. Note that, due to its simplicity, the "baseline" approach is widely used in HVAC management. With such an approach, the setpoint temperature value is chosen to be at the lower boundary of the thermal comfort zone during occupancy periods whereas the "night setback" mode is applied during innocupancy [5].

Advanced scheduling techniques can also be considered in HVAC management. So, Lee and Braun used short-term measurement data to determine demand-limiting control

*Corresponding author
Email address: stephane.grieu@promes.cnrs.fr (**Stéphane Grieu**)

setpoint trajectories [6]. The authors developed three different methods, named "Semi-Analytical" (SA), "Exponential setpoint equation-based Semi-Analytical" (ESA), and "Load Weighted-Averaging" (LWA) methods, respectively. Each method gives an estimate of a building-specific setpoint trajectory that gives a "flat" cooling load profile during a specified demand-limiting period [7]. Another possible technique is the "5-period division" scheduling [8]. Using this technique, the day is divided into five periods, according to occupancy, with specific operation in each period. One can also talk about the "extended precooling with zone temperature reset" technique [9]. Such an approach is based on varying the temperature setpoints and shifting the heating/cooling loads from daytime to night time [10]. The last advanced scheduling technique one can highlight is the "agressive duty cycling" technique [11]. Based on occupancy, the HVAC system is turned on and off many times in a day and, as a result, an efficient real-time detection of people is needed.

One can also highlight efficient approaches based on artificial intelligence tools. In Ref. [12], Gouda et al. proposed an efficient fuzzy controller for HVAC systems by taking into account a wide range of human comfort criteria in the control action formulation. In Ref. [13], Dounis and Caraiscos developed a multi-agent control system in order to manage air quality as well as thermal and illuminance comfort. As another interesting approach, Bermejo et al. designed a thermal comfort adaptive system based on fuzzy logic and on-line learning [14]. In most cases, these approaches require to turn the HVAC system on then off at fixed times. Consequently, this can impact thermal comfort negatively if the system is started too late or energy consumption if triggering happens too soon.

Another interesting option in HVAC management lies in considering predictive control techniques. As it has been highlighted by many other studies, these advanced techniques can take advantage of the intermittent use of non-residential buildings and allows the behaviour of the considered system to be anticipated [15]. In this sense, Paris et al. developed a Model Predictive Controller (MPC) in order to control indoor temperature and minimize energy consumption in multi-energy buildings [16]. In Ref. [17], Moroşan et al. proposed a distributed predictive approach to control several areas simultaneously, while taking into account thermal transfers. In this approach, thermal comfort is defined on the basis of a reference temperature. The proposed algorithm is useful but on-line optimization is needed and computation time is extensive. Because predictive control is well adapted to the management of energy resources, we recently developed a new approach allowing energy consumption to be significantly reduced and the HVAC subsystems of a non-residential building to be turned on and off at the right time [18]. Only heating was considered. We used the Predicted Mean Vote (PMV) index as a thermal comfort indicator and focused on satisfying constraints. The algorithm we developed offers very good performance and does not require on-line optimization. As a result, it is computationnaly tractable and can be implemented in an embedded system with limited resources. Its main drawback lies in the simultaneous engaging and stop of all of the HVAC subsystems. That is why the present paper focuses on improving this predicitive approach by optimizing for each room of the building the operation time of its HVAC subsystem. Both heating and cooling modes are now considered. We decided for a Genetic Algorithm (GA) so as to solve the optimization problem [19] and used feedforward (multi-layer) artificial neural networks trained with the cascade-correlation algorithm to develop the controller's internal models. Note that genetic algorithms have been already used in energy resources and thermal comfort management. In Ref. [20], Attia et al. reviewed the current trends in simulation-based Building Performance Optimisation (BPO) and outlined criteria for both the selection and evaluation of optimization tools, including evolutionary algorithms. In Refs. [21, 22], thermal comfort is managed into a unique room by using a genetic algorithm, without considering heat transfer with the other rooms in the building. Note that Liu et al. also used this kind of algorithm to optimize HVAC operation by searching for optimal control settings [23].

The present paper is organized as follows: Section 2 is about the non-residential building we modelled thanks to the EnergyPlus software. This building is located in Perpignan (France). In Section 3, the Predicted Mean Vote (PMV) is defined. We used it as a thermal comfort indicator. Next, the predictive strategy as well as the low-order ANN-based models we developed and used as controller's internal models are described (Section 4). Finally, the simulation results we obtained in both heating and cooling modes are analyzed and compared with the results given by basic scheduling techniques (Section 5). The paper ends with a conclusion and an outlook to future work.

2. Non-residential building

In order for the proposed strategy to be evaluated, the thermal behaviour of a real non-residential building has been modelled using the EnergyPlus software, which is able to perform accurate building simulations.

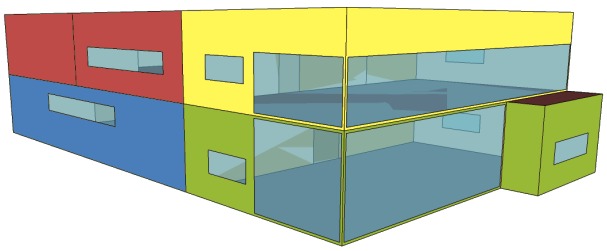

Figure 1: Topology of the non-residential building located in Perpignan. The green, yellow, red and blue areas are for offices in the ground floor (R1), offices in the first floor (R2), a manufacturing area (R3) and a warehouse (R4), respectively.

The building is a $1000\,\mathrm{m}^2$ two-storey structure, built in 2008 and located in Perpignan (France). It is facing south

Table 1: Properties of the materials used in the exterior walls of the building.

Material	Brick	Heavy weight concrete	Insulation board	Gypsum board
Thickness (cm)	10	20	5	2
Thermal conductivity ($\mathrm{W\,m^{-1}\,K^{-1}}$)	0.89	1.45	0.03	0.16
Density ($\mathrm{kg\,m^{-3}}$)	1920	2000	43	800
Specific heat ($\mathrm{J\,kg^{-1}\,K^{-1}}$)	790	1000	1210	1090

and agrees with the French Thermal Regulation of year 2005. About a dozen employees work in the offices at the ground and first floors (the green and yellow areas in Fig. 1, R1, R2). The red area in the first floor (R3) is a manufacturing area where six persons work seated or in a standing position. This room is composed of an open space of $230\,\mathrm{m^2}$ and three unheated storage rooms of $110\,\mathrm{m^2}$. The last room in the ground floor is a warehouse (the blue area in Fig. 1, R4) which is not heated. For both the warehouse and the manufacturing area, ceiling height is 3.90 m. In the offices, a suspended ceiling stands at 2.70 m. All the materials used in the building as well as their main properties are listed in Table 1. For each material, its thickness (cm), thermal conductivity ($\mathrm{W\,m^{-1}\,K^{-1}}$), density ($\mathrm{kg\,m^{-3}}$), and specific heat ($\mathrm{J\,kg^{-1}\,K^{-1}}$) are given. The exterior walls consist in several layers. From the outside to the inside, a brick layer, heavy weight concrete, an insulation board, and a gypsum board are juxtaposed. The interior walls are composed of two gypsum boards, for a total thermal resistivity of 2.2 $\mathrm{m^2\,K\,W^{-1}}$. The south face and a part of the west face of the building are made of glass. Note that glass is treated to filter infrared radiation. This avoid overheating in summer. The other glasses in the building consist in 3 mm double glazed bays.

The present study focuses on managing the HVAC subsystems in the three following rooms of the building: the offices on both floors (R1, R2) and the manufacturing area (R3). These rooms are equipped with air and radiant temperature sensors. Note that no heat transfer between the warehouse (R4) and the other rooms is explicitely taken into account (considered as a system disturbance). Heating is handled by a zoned electrical HVAC system consisting in several subsystems, one for each area, where only the temperature set-points can be adjusted. Each subsystem is managed by a local controller. All units have a coefficient of performance equal to 3.8. The characteristics of the rooms R1, R2, R3 and R4 are listed in Table 2.

Table 2: Characteristics of the rooms R1, R2, R3 and R4.

Room	R1	R2	R3	R4
Surface ($\mathrm{m^2}$)	165	155	230	340
Volume ($\mathrm{m^3}$)	450	420	900	1330
Heating power (kW)	5	5	10	n/a
Number of occupants (-)	8	5	6	n/a
Metabolic activity ($\mathrm{W\,m^{-2}}$)	70	70	116	n/a
Lighting power (kW)	1	1	1.4	n/a

As previously stated in the paper (Section 1), the proposed management strategy is based on a model predictive controller that will supervise the HVAC subsystems and optimize their operation times (Fig. 2).

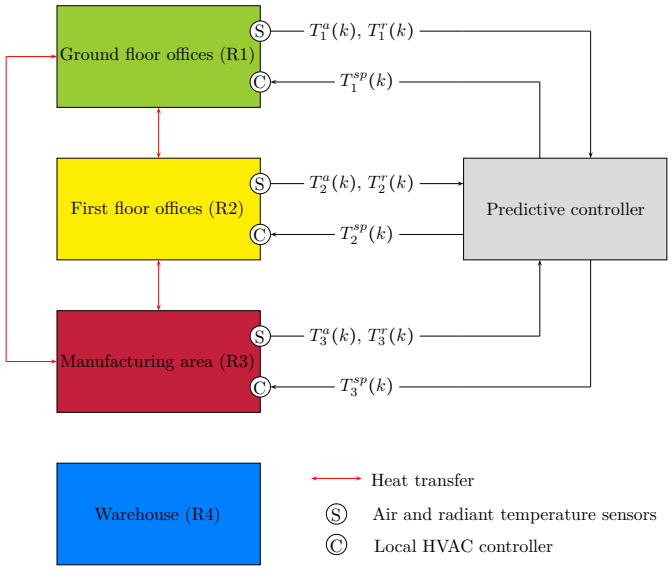

Figure 2: The three rooms in the building (R1, R2 and R3) equipped with air and radiant temperature sensors (T_j^a and T_j^r, $\forall j \in [\![1;3]\!]$) and controlled HVAC subsystems. The warehouse (R4) is unheated. No heat transfer between the warehouse and the other rooms of the building is explicitely taken into account. T_j^{sp}, $\forall j \in [\![1;3]\!]$, is the HVAC temperature set-point in the room j.

3. Thermal comfort

The Predicted Mean Vote (PMV) index is used as a thermal comfort indicator. It has been developed by Fanger in 1973 [24], before to be standardized by international organizations. The PMV index allows the thermal sensation felt by people in a room to be evaluated. This sensation is described by a scale ranging from -3 to +3. 0 is for a neutral thermal sensation, which is often associated with the state of (thermal) comfort (Table 3). The exchange of heat between the human body and its surroundings strongly governs thermal comfort. It is highly subjective and can be considered as perfect when the sum of exchanges is zero. The PMV index is computed as follows, in the room j, $\forall j \in [\![1;3]\!]$ (1):

$$PMV_j = [0.303exp^{-0.036M_j} + 0.028] \times L_j \quad (1)$$

with L_j the difference between the heat produced and the heat lost (2):

$$L_j = M_j - W_j - H_{j,1} - H_{j,2} - H_{j,3} - H_{j,4} - H_{j,5} - H_{j,6} \quad (2)$$

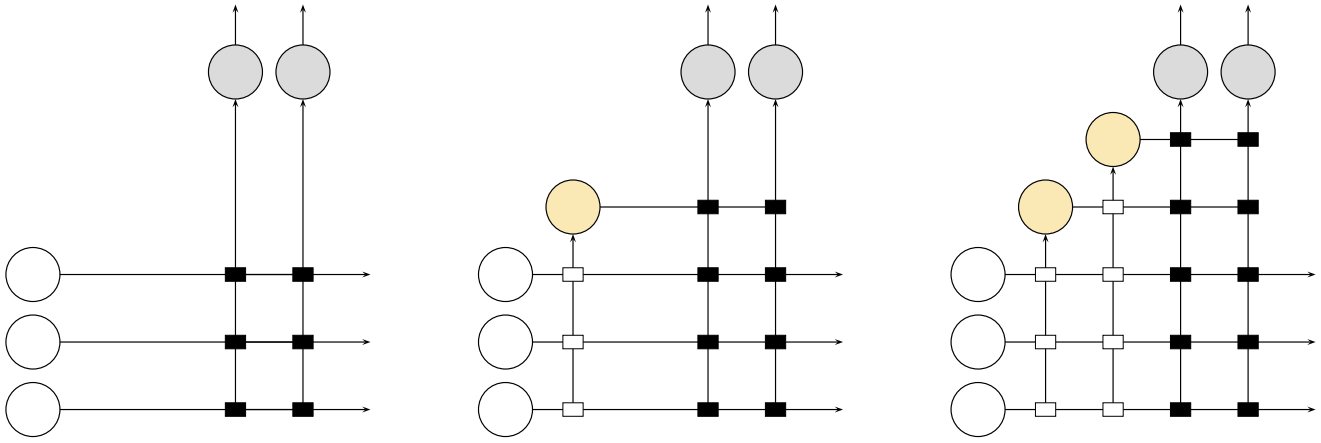

Network's initial topology (no hidden neuron) | Network with one neuron in its hidden layer | Network with two neurons in its hidden layer

Figure 3: The cascade-correlation algorithm. White, beige and grey circles deal with inputs, hidden neurons and output neurons, respectively. Black rectangles depict weighted connections between inputs and output neurons or between hidden neurons and output neurons. White rectangles depict weighted connections between inputs and hidden neurons or between hidden neurons.

M_j is the metabolism and W_j is the external work. $H_{j,1}, ..., H_{j,6}$ are the heat loss coefficients ($\mathrm{W\,m^{-2}}$). $H_{j,1}$ is the heat loss by diffusion through the skin and $H_{j,2}$ is the heat loss by sweating. $H_{j,3}$ and $H_{j,4}$ are the losses by latent and dry respiration, respectively. Finally, $H_{j,5}$ is the heat loss by radiance and $H_{j,6}$ is the heat loss by convection. To calculate these heat loss coefficients, several parameters about environment and occupants are taken into account, $\forall j \in [\![1;3]\!]$: air temperature ($T_j^a$), radiative temperature (T_j^r), relative humidity (HR_j), air speed (v_j^a), metabolic activity, and clothing thermal insulation (ICL_j). Note that air speed is not taken into account in the EnergyPlus software. However, this missing information is not critical at all because air speed has no influence on the PMV index as long as it remains below $0.1\,\mathrm{m\,s^{-1}}$. This is mostly the case within the considered non-residential building. Moreover, metabolic activity is supposed to be constant and only depends on the room.

Table 3: Thermal sensation scale.

PMV value	Thermal sensation
+3	Hot
+2	Warm
+1	Slightly warm
0	Neutral
-1	Slightly cool
-2	Cool
-3	Cold

In offices (R1 and R2), people work most of the time in a sitting position and, as a result, M_j, $\forall j \in [\![1;3]\!]$, is set to $70\,\mathrm{W\,m^{-2}}$ (i.e. 1.2 met). Activity in the manufacturing area (R3) is much more dynamic and M_j is set higher to $116\,\mathrm{W\,m^{-2}}$ (i.e. 2 met). Moreover, depending on outdoor temperature, people dress differently. Consequently, clothing thermal insulation in the room j (ICL_j), $\forall j \in [\![1;3]\!]$, varies over time [25]. It is defined, each day, from the outdoor temperature observed at 6 a.m., noted t_6 (Table 4). Usual clothes for summer are a pant with a short-sleeved shirt, whereas during winter, usual clothes are a trouser with a long-sleeved shirt.

Table 4: Clothing thermal insulation.

Outdoor temperature at 6 a.m.	ICL_j (clo)
$t_6 < -5°\mathrm{C}$	1
$-5°\mathrm{C} \leq t_6 < 5°\mathrm{C}$	$0.818 - 0.0364 t_6$
$5°\mathrm{C} \leq t_6 < 26°\mathrm{C}$	$10^{-0.1635-0.0066 t_6}$
$t_6 \geq 26°\mathrm{C}$	0.46

4. Multizone predictive control

As previously mentioned in the paper, each room in the non-residential building has its own HVAC subsystem, handled by a local controller (Fig. 2). Simulation is carried out using the EnergyPlus building model we developed and the predicitive control strategy is implemented thanks to Matlab®. The MLE + interface enables both tools to communicate in real time [26]. As a key point, we used feedforward neural networks trained with the cascade-correlation algorithm in order to develop the controller's internal models. Hidden and output neurons use sigmoid and linear activation functions, respectively.

4.1. The cascade-correlation algorithm

During the past decade, artificial neural networks have been widely used to solve complex real-world problems. A key point when using such tools is to find the appropriate topology of the network used to solve a given problem (basically, the number of hidden layers as well as the number of units, or neurons, to be put on them) and, secondly, to optimize its parameters using training examples. Training aims at establishing a satisfactory relationship between

input and output patterns. The cascade-correlation algorithm [27] is an adaptive (or constructive) learning algorithm used with self-growing feedforward neural networks (with one hidden layer only, what proved to be enough to approximate a large class of functions) [28]. Compared with a neural network trained with the conventional backpropagation algorithm [29], a cascade-correlation neural network does not have a fixed size (i.e. a fixed number of units in its hidden layer). A cascade-correlation neural network grows from an initial topology with no hidden units. So, each input is connected to each output neuron and the network is trained using learning data (training examples). These data have to be fully representative of all the features the network is intended to learn. When there is no significant reduction in the approximation error, the training phase is terminated and all the weights obtained are frozen. Then, hidden units will be dynamically added and trained one by one until a given performance criterion is satisfied (Fig. 3). Usually, a new hidden neuron is chosen from a pool of candidates with different initial weights. The new hidden units are so cascaded with the neural network inputs as well as existing hidden units. During the training process, the weights affected to the connections between these new units and both the network's inputs and preexisting hidden units ("input" weights) are adjusted by maximizing C, which is the sum over all the network's output neurons of the magnitude of the correlation between V_p, the value of the candidate unit for example p, and $E_{p,o}$, the residual output error measured at neuron o. A gradient ascent is performed in order to maximize C, with C formulated in the following way (3):

$$C = \sum_{o} \left| \sum_{p} (V_p - \bar{V})(E_{p,o} - \bar{E_o}) \right| \tag{3}$$

$\bar{V}$ and $\bar{E_o}$ are the respective averaged values of V and E_o over all the training examples. In order to maximize C (3), the partial derivative of C with respect to each of the incoming weigths of the candidates (w_i) has to be computed. $\partial C/\partial w_i$ can be expressed as follows (4):

$$\partial C/\partial w_i = \sum_{p,o} \sigma_o (E_{p,o} - \bar{E_o}) f'_p I_{i,p} \tag{4}$$

σ_o is the the correlation between the value of the candidate unit and output o, f'_p is the derivative of the candidate's activation function with respect to the sum of its inputs (for example p), $I_{i,p}$ is the input received by the candidate unit from unit i (for example p). When the process discribed above is finished, the adjusted "input" weights are also frozen. Weights affected to the connections between the new hidden units and output neurons (called "output weights") are further updated using the above-mentioned backpropagation algorithm with the aim of minimizing the network output error. This iterative procedure is of involving more and more hidden neurons and is repeated so as to achieve a good approximation performance [30].

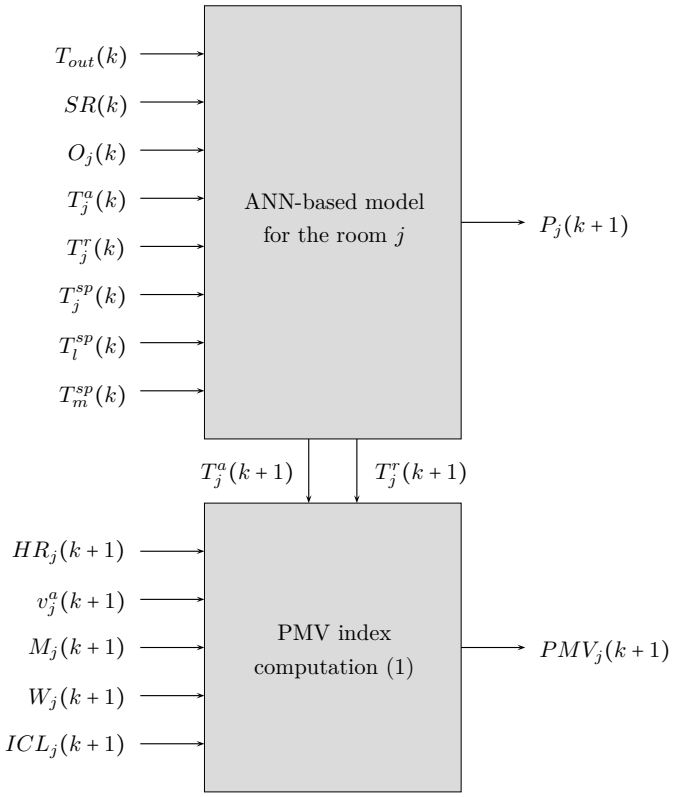

Figure 4: ANN-based model for the room j, $\forall j, l, m \in [\![1;3]\!]$ such as $j \neq l \neq m$. PMV_j is computed at time step $k+1$ using (1) (Section 3, heating or cooling mode).

4.2. Low-order ANN-based models

We used a total of six feedforward (self-growing) artificial neural networks so as to model at time step $k+1$, $\forall j \in [\![1;3]\!]$, the air ($T_j^a$) and radiative ($T_j^r$) temperatures (5 and 6) as well as the electrical power consumed by the HVAC subsystems (P_j) (7), for both operation modes (heating and cooling) and the three considered rooms in the non-residential building (i.e. the offices on both floors and the manufacturing area). At time step k, estimation is carried out from the following inputs: outdoor temperature (T_{out}), solar radiation (SR), room occupancy (O_j), T_j^a, T_j^r, T_j^{sp}, and the HVAC temperature set-points in the two adjacent rooms (T_l^{sp} and T_m^{sp}) of room j, $\forall j, l, m \in [\![1;3]\!]$ such as $j \neq l \neq m$ (Fig. 4). We identified all the parameters and found the optimal topologies of the ANN-based models through a training phase, resorting to the cascade-correlation algorithm as well as data generated by the EnergyPlus model of the non-residential building:

$$\begin{aligned} T_j^a(k+1) = f_j^1 \big(&T_{out}(k), SR(k), O_j(k), \dots \\ &T_j^a(k), T_j^r(k), T_j^{sp}(k), T_l^{sp}(k), T_m^{sp}(k)\big) \end{aligned} \tag{5}$$

$$\begin{aligned} T_j^r(k+1) = f_j^2 \big(&T_{out}(k), SR(k), O_j(k), \dots \\ &T_j^a(k), T_j^r(k), T_j^{sp}(k), T_l^{sp}(k), T_m^{sp}(k)\big) \end{aligned} \tag{6}$$

$$\begin{aligned} P_j(k+1) = f_j^3 \big(&T_{out}(k), SR(k), O_j(k), \dots \\ &T_j^a(k), T_j^r(k), T_j^{sp}(k), T_l^{sp}(k), T_m^{sp}(k)\big) \end{aligned} \tag{7}$$

Depending on the neural model to be developed, the cascade-correlation algorithm decided for 18 to 24 hidden neurons. Validation has been carried out using a 2-month database and we obtained correlation coefficients higher than 0.9 and mean relative errors lower than 5%, whatever the operation mode (heating or cooling) and the room (R1, R2 or R3). Fig. **??** shows some of the results we obtained, for the ground floor offices and a period of five winter days. The black line is for values provided by the EnergyPlus software whereas the red line deals with estimated values. Using (1) (see Section 3), $PMV_j(k+1)$, $\forall j \in [\![1;3]\!]$, is computed among others from $T_j^a(k+1)$ and $T_j^r(k+1)$ (see Fig. 4). Note that M_j and HR_j are supposed to be constant over the simulation period (i.e. from June 1 to September 30 then from November 1 to March 31, 2011) and over the forecast horizon, respectively. ICL_j is computed from t_6 (Table 4) and considered as constant from 6 a.m. (day d) to 6 a.m. (day $d+1$). In addition, it is the same whatever the room. Finally, v_j^a and W_j are supposed to be null. As previsouly stated in the paper, we used the developed ANN-based models as controller's internal models.

4.3. Control strategy

Fig. 5 depicts the predictive control strategy we developed first to search for the right time t_j to turn the HVAC subsystem on then off in the room j, $\forall j \in [\![1;3]\!]$, with the aim of minimizing the total consumption of electrical power (8). The strategy also deals with the temperature set-point $\tilde{T}_j^{sp}$ allowing thermal comfort constraints to be met during occupancy periods (i.e. leading to $PMV_j^{sp} = 0$). $\bar{t}$ is about the optimal switching times (integer values) for the three HVAC subsystems we considered in the non-residential building:

$$J^\star = \min_{\bar{t}\in\mathbb{N}} \left(J(\bar{t}) = \sum_{k=1}^{p} \sum_{j=1}^{3} \left(P_j(t_j,k)\right) \right) \tag{8}$$

$$\begin{cases} \bar{t}_0 < \bar{t} < \bar{t}_p, \text{ with } \bar{t} = [t_1\, t_2\, t_3] \text{ and } p \text{ the forecast horizon} \\ PMV_j^{min} < PMV_j(k) < PMV_j^{max}, \forall O_j(k) \neq 0, \forall j \in [\![1;3]\!] \end{cases}$$

PMV_j^{min} and PMV_j^{max} are thermal comfort thresholds defined for the room j, $\forall j \in [\![1;3]\!]$. These thresholds can be adapted in order to meet users' needs and preferences. For the simulations, we decided for $PMV_j^{min} = -0.5$ and $PMV_j^{max} = 0.5$. In addition, outdoor temperature (T_{out}) and solar radiation (SR) have been forecasted over an horizon (p) of 8 hours, using previous day values corrected by current values (9 and 10). Room occupancy (O_j) is known in advance:

$$\begin{aligned} T_{out}(k+p) = T_{out}(k+p-24\text{h}) + T_{out}(k)\ldots \\ - T_{out}(k-24\text{h}) \end{aligned} \tag{9}$$

$$SR(k+p) = SR(k+p-24\text{h}) \tag{10}$$

Finally, T_j^{sp} (the HVAC temperature set-point in the room j) is set by the decision block (Fig. 5), according to t_j and $\tilde{T}_j^{sp}$, $\forall j \in [\![1;3]\!]$.

4.4. Genetic algorithm for problem resolution

4.4.1. Overview

In order to solve the problem formulated in Section 4.3 (i.e. minimizing electrical power consumption in the non-residential building while meeting thermal constraints by turning the HVAC subsystems on then off at the right time), we decided for a numerical optimizer able to deal with integer values and known to be efficient in the search for the optimal solution (or an acceptable solution in its immediate neighbourhood), by testing a raisonable number of possible solutions. As a consequence, we used the Genetic Algorithm (GA) from the Matlab® Global Optimization Toolbox [31]. As it is well known, GAs are methods for solving constrained and unconstrained optimization problems based on a natural selection process that mimics biological evolution (Darwin's natural selection hypothesis). GAs are theoretically and empirically proven to provide robust searches in complex spaces. In particular, an objective function can be minimized using a genetic algorithm without calculating derivatives (analytical approaches based on gradient calculation are restricted to the estimation of uncorrelated parameters). GAs are also recognized for their robustness. Due to their probabilistic nature, the incidence of the initial guess on the optimization process effectiveness is low. In addition, GAs produce not just one optimal individual (solution) but a population of good individuals. However, GAs have some drawbacks. In particular, they can be slow to converge in case of complex and hard-to-solve problems. As a result, significant response times make sometimes their use in real-time applications not possible. GAs may also be less efficient and slower than traditional optimization methods in case of very simple problems.

4.4.2. Optimization process

At each step of the process, the best individuals are selected from the current population (the initial population is randomly generated) and serve as parents in order to produce the children for the next generation. Each individual in the population is a vector $\bar{t} = [t_1\, t_2\, t_3]$. Selection is based on performance (typically, the genetic algorithm is more likely to select parents with better fitness values), that is why the thermal behaviour of the three considered rooms (R1, R2 and R3) in the non-residential building is simulated for each individual in the population. Over successive generations, this population evolves toward an optimal solution $\bar{t}_{opt}$ allowing both the consumption of electrical power in the room j to be minimized ($P_j, \forall j \in [\![1;3]\!]$) and the thermal constraints to be met. As a key point, we performed crossover (i.e. recombinations of individuals) and mutation (i.e. random alterations of individuals) operations during the optimization process [32, 33]. Crossover has been achieved thanks to the "scattered" technique, using a randomly-generated binary vector in order to select and combine some of the "genes" of two parents and form a child. We quantified the impact of the crossover fraction (C), which is about the part of a given population

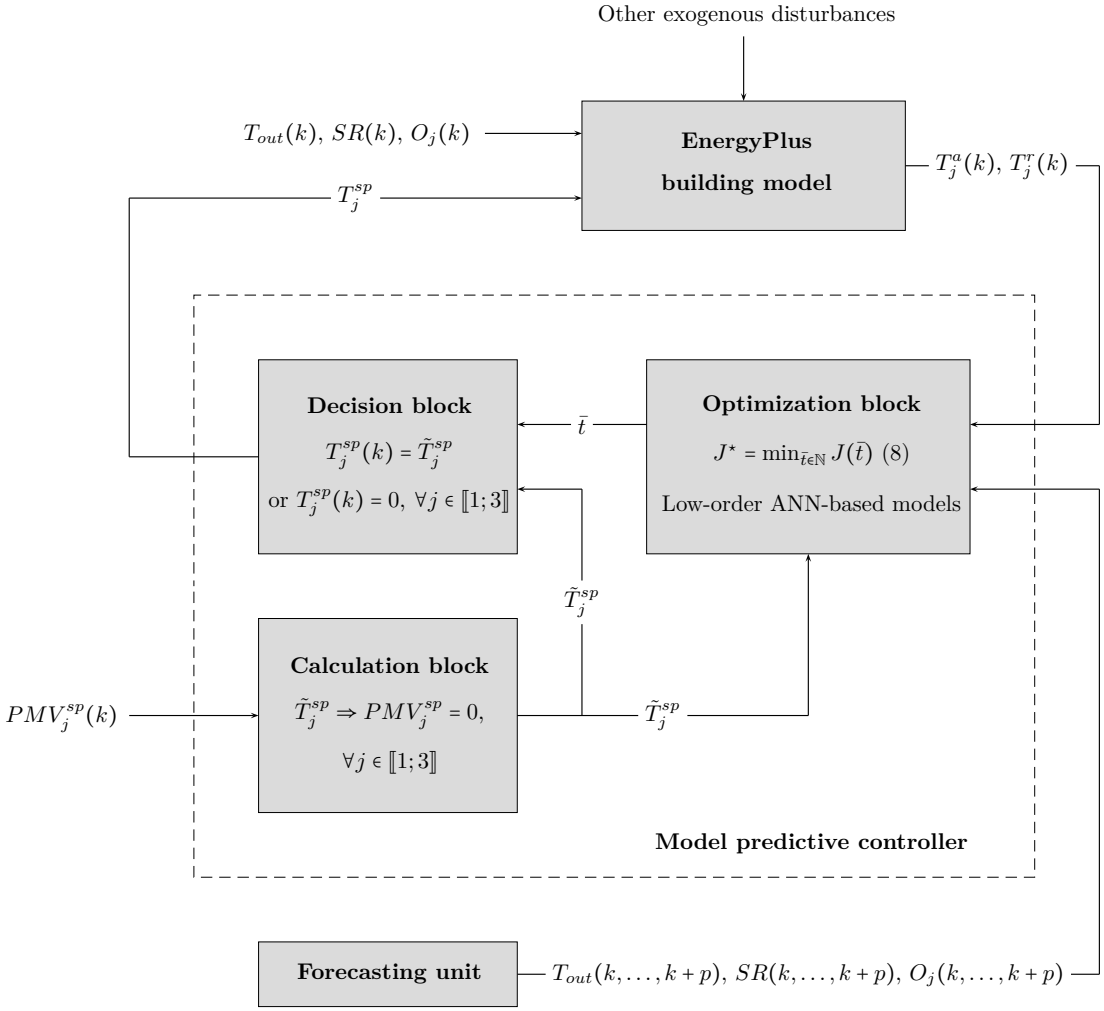

Figure 5: Block diagram of the predictive control strategy. See Sections 3 and 4 for a description of the parameters involved in the strategy.

that is made up of crossover children, on performance. Mutation consists in adding a random number to each component of a given parent vector. So, we considered a Gaussian distribution with mean zero and controled the average amount of mutation applied to a parent in each generation (i.e. the rate at which the average amount of mutation (M) decreases (linearly) during the optimization process). Crossover is the main exploratory device of genetic algorithms when mutation increases the variability of a given population of individuals. Mutation can be seen as a random explore and leads to a "jump" in the location of the generated solutions whereas crossover produces a more controlled move. Searching for the adequate values of C and M aims to favour convergence as well as limit the risk of falling and being trapped into a local minimum during the optimization process. This process ends if the maximum number of generations is reached or the solution found is not improved for ten successive generations. The parametric analysis we performed also allowed the impact on performance of both the population size and the number of successive generations to be highlighted. Note that, whatever the crossover fraction (C) and the average amount of mutation (M), the higher both the number of individuals in the population and the number of generations are, the higher the percentage of optimal solutions is (in relation to the minimization of P_j, $\forall j \in [\![1;3]\!]$, while meeting the thermal constraints). Of course, the resolution time increases with the population size and the number of successive generations. As a result, we searched for the best compromise so as to reach a satisfactory solution in a reasonable amount of time. Clearly, a too low crossover fraction (C) slows down the optimization process. With C equal to 0.25, acceptable results can be obtained only in case of many individuals in the population and if many successive generations are performed. One can also note that a crossover fraction close to 1 impacts convergence negatively. In addition, in that case, overconsumption of electrical power is high. As another interesting point, the average amount of mutation (M) seems to be less impactful than the crossover fraction (C). Finally, on the basis of all these factual elements, we decided for 25 individuals in the population, 40 successive generations, and a crossover

fraction/average amount of mutation equal to 0.5 (Table 5). With such a configuration, overconsumption of electrical power is insignificant whereas the number of solutions to be tested is rather limited. As a consequence, resolution time is moderate.

Table 5: Optimal configuration for problem resolution.

Feature	Value
Individuals in the population	25
Successive generations	40
Crossover fraction (C)	0.5
Average amount of mutation (M)	0.5

5. HVAC operation

5.1. Non-predictive strategies

We considered five non-predictive strategies, including four basic scheduling techniques [3], in order to highlight the benefits of the predictive approach developed for non-residential buildings equipped with multizone HVAC systems. The first technique (strategy S1) is the simplest of all techniques: the subsystems operate all the time, including during non-occupancy periods (Fig. 6). The second technique (strategy S2) is based on a scheduler used to stop the HVAC subsystems during periods of non-occupancy and to turn them on in the morning, two hours before people arrive at the building (i.e. at 6 a.m.). The subsystems are turned off when people leave (i.e. at 6 p.m.). S2 is the technique currently used in the real non-residential building located in Perpignan (south of France) and modelled using the EnergyPlus software (Fig. 7). The third scheduling technique we considered (strategy S3) is the "Early Switch-Off" (ESO) technique. Remember that using the ESO technique, the HVAC subsystems are turned off two hours before people leave the building (i.e. at 4 p.m.) (Fig. 8). The next basic technique (strategy S4) is based on the "Alternate Switch-On/Off" (ASOO) technique. Using such a technique, the HVAC subsystems are alternatively switched on and off [4]. In that case, the subsystems are one hour on and one hour off between 6 a.m. and 5 p.m. (Fig. 9). The last basic scheduling technique we considered is the "pre-heating (or pre-cooling) in the Demand Reduction" (DR) technique (strategy S5). S5 is about pre-heating or pre-cooling a building during off-peak periods (Fig. 10). With such a strategy, the HVAC subsystems operate between 5 a.m. and 7 a.m. (pre-heating or pre-cooling time) but do not operate between 7 a.m. and 8 a.m. then between 12 p.m. and 1 p.m. (i.e. during the lunch break). Whatever the non-predictive strategy (S1, S2, S3, S4 or S5), $T_j^{sp} = 22°\text{C}$, $\forall j \in [\![1;3]\!]$ (even during non-occupancy periods if S1 is considered). Remember that, unlike the basic scheduling techniques, the proposed predictive strategy allows the right time to turn the HVAC subsystems on then off to be found in each of the considered rooms of the building while meeting with thermal comfort requirements (strategy S6). As a result, consumption of electrical power can be significantly reduced.

5.2. Analysis of the results

5.2.1. Overall results

In order to evaluate performance regarding thermal comfort, we considered the percentage of time for which the PMV value is out of the desired interval during occupancy periods $[-0.5;+0.5]$ (discomfort criterion). Moreover, an average value (per day and square meter) is used for energy consumption. Tables 6 and 7 summarize the results we obtained for two simulation periods, from November 1 to March 31 (heating mode) and from June 1 to September 30, 2011 (cooling mode). First, one can clearly observe that applying S1 to the three considered HVAC subsystems leads to high energy consumption, whatever the operation mode. In addition, thermal comfort is rather bad in winter time (heating mode). Taking S2 as the reference strategy, one can also observe that with the "Early Switch-Off" (ESO) or the "Alternate Switch-On/Off" (ASOO) technique, energy consumption is significantly reduced, whatever the operation mode, but thermal comfort is worse (especially during the hottest period of the year). In heating mode (from November 1 to March 31, 2011), energy consumption is reduced from 80.9 to 54.2 Wh/day m^2 (-33%) with S3 (ESO) and from 80.9 to 59.5 Wh/day m^2 (-26%) with S4 (ASOO). In cooling mode (from June 1 to September 30, 2011), energy consumption is reduced from 122.6 to 96.7 Wh/day m^2 (-21%) with S3 (ESO) and from 122.6 to 90.5 Wh/day m^2 (-26%) with S4 (ASOO). However thermal comfort is clearly degraded during this period of the year: 0.2% (S2) vs. 13.4% (S3) or 25.4% (S4). Using S4, the way the HVAC subsystems are managed leads to significant changes in the PMV index and, as a result, thermal discomfort is high. In addition, switching on and off the subsystems many times a day impacts on lifetime. The last basic strategy (S5) we tested is based on the "Pre-heating (pre-cooling) in the Demand Reduction" (DR) scheduling technique. As one can see in Tables 7 and 6, S2 (the technique currently used in the real non-residential building) and S5 provide very close performance, whatever the operation mode (heating or cooling). During the coldest period of the year (from November 1 to March 31, 2011), energy consumption is 80.9 Wh/day m^2 with S2 and 81.0 Wh/day m^2 with S5. Thermal comfort is also similar (slightly better with S2): 14.4% (S2) vs. 16.5% (S5). In cooling mode (from June 1 to September 30, 2011), performance of S5 is slightly better than performance of S2. Energy consumption is reduced of about 2%, from 122.6 Wh/day m^2 to 119.8 Wh/day m^2, and thermal discomfort is similar (0.2% (S2) vs. 0.1% (S5)). Finally, the predictive strategy (S6) allows energy consumption to be reduced and thermal comfort to be improved in a significant way, whatever the period of the year, in comparison to what can be observed with S2. In heating mode, energy consumption and thermal discomfort are reduced from 80.9 to 69 Wh/day m^2 (-15%) and from 14.4 to 6.4% (-56%), respectively. In cooling mode, both are reduced from 122.6 to 116.2 Wh/day m^2 (-5%) and from 0.2 to 0.1%

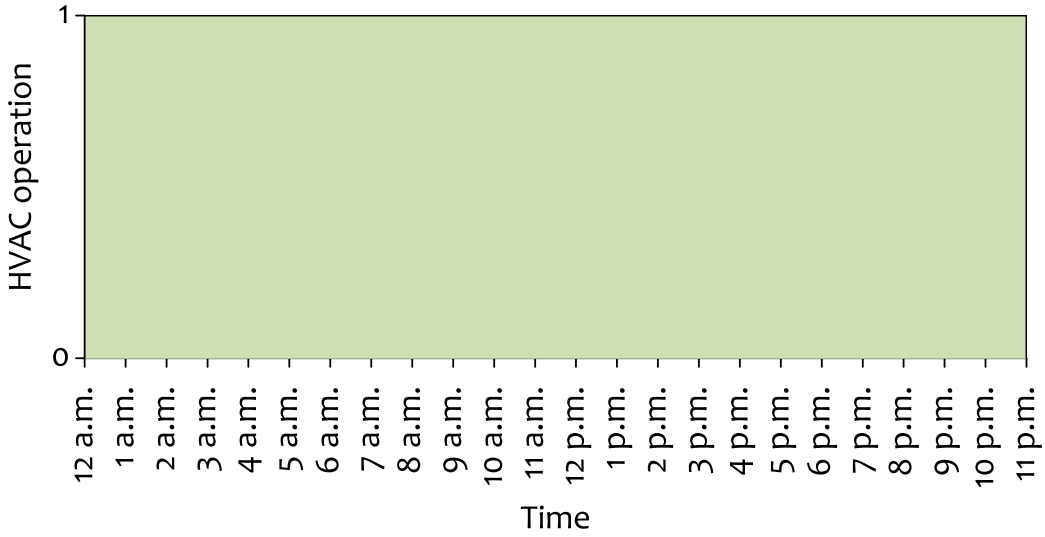

Figure 6: Daily HVAC operation (S1). 0 is for non-operating HVAC subsystems, 1 is for subsystems in operation.

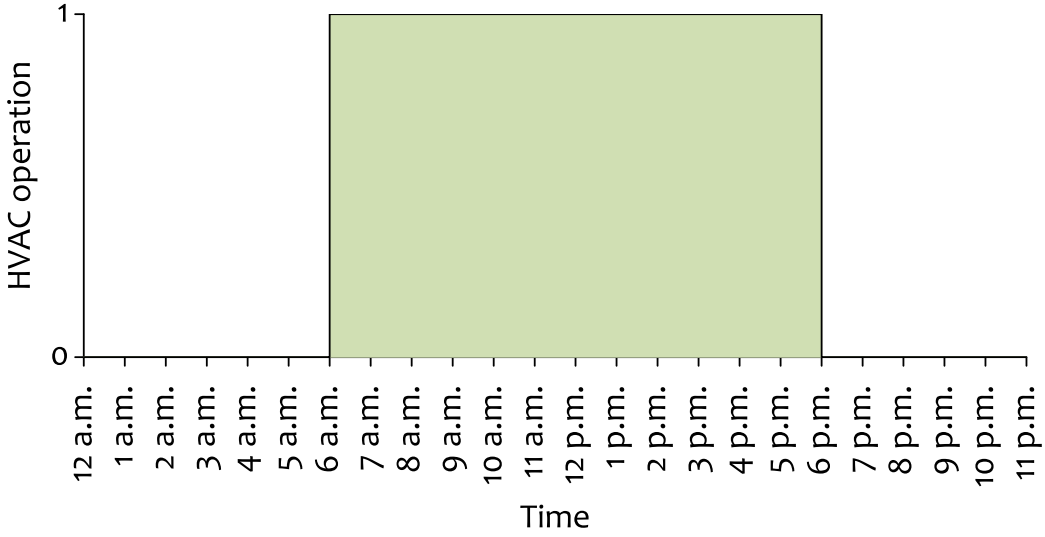

Figure 7: Daily HVAC operation (S2). 0 is for non-operating HVAC subsystems, 1 is for subsystems in operation.

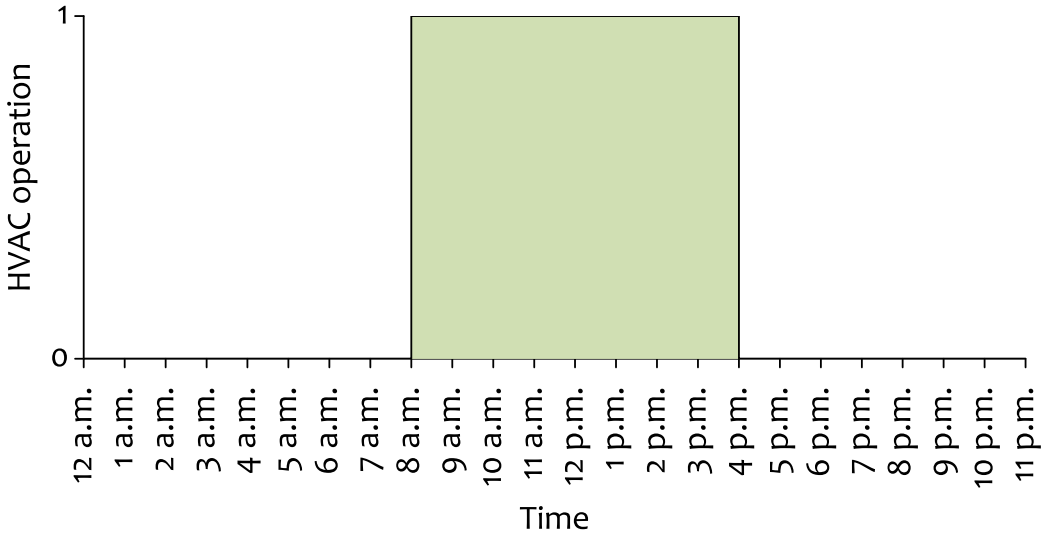

Figure 8: Daily HVAC operation (S3). 0 is for non-operating HVAC subsystems, 1 is for subsystems in operation.

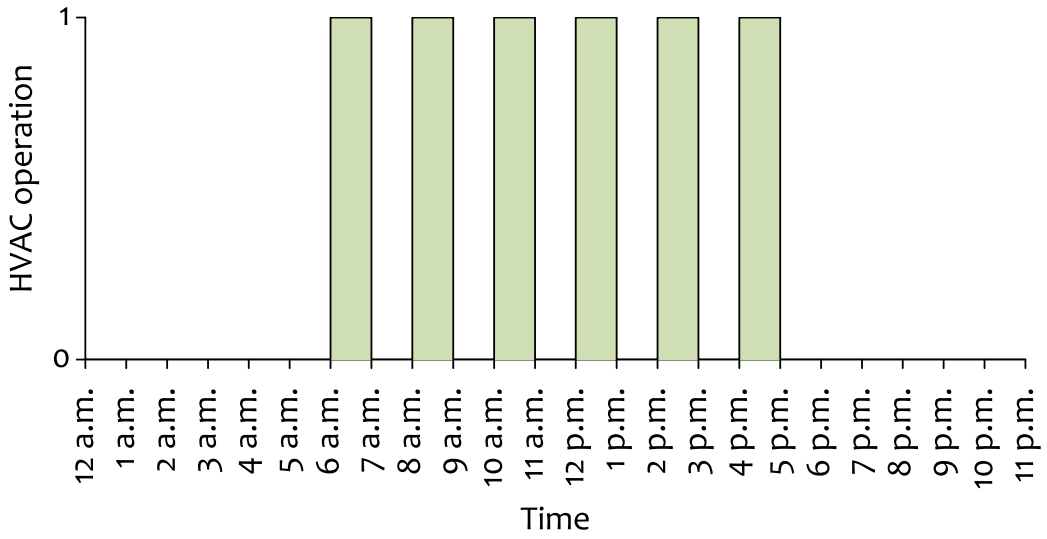

Figure 9: Daily HVAC operation (S4). 0 is for non-operating HVAC subsystems, 1 is for subsystems in operation.

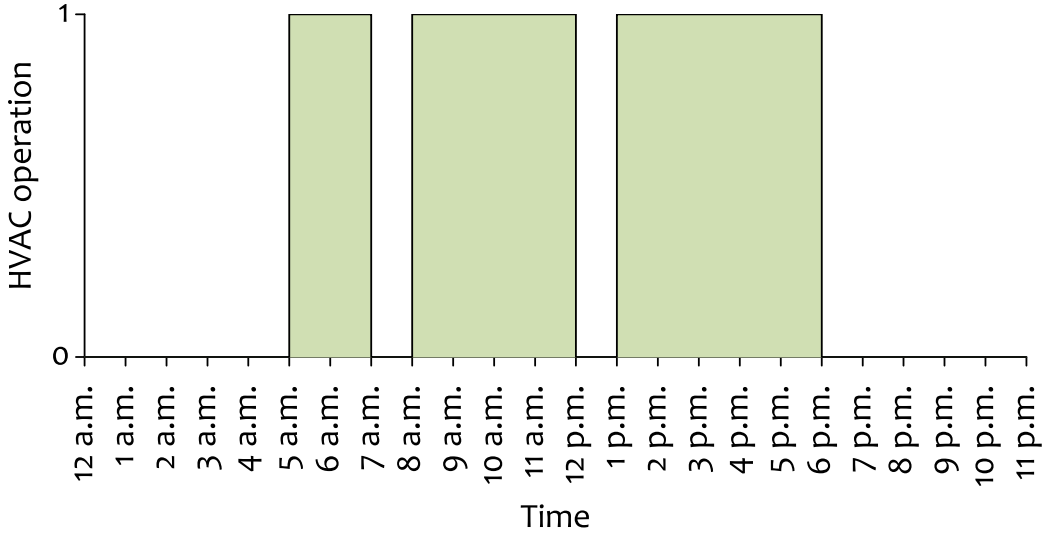

Figure 10: Daily HVAC operation (S5). 0 is for non-operating HVAC subsystems, 1 is for subsystems in operation.

Table 6: Performance of the different strategies, $\forall j \in [\![1;3]\!]$. The simulation period is from November 1 to March 31, 2011 (heating mode).

	Occupancy period	Non-occupancy period	Consumption (Wh/day m^2)	Discomfort criterion
S1	$T_j^{sp} = 22°C$	$T_j^{sp} = 22°C$	209.5	19.4%
S2	$T_j^{sp} = 22°C$	Off	80.9	14.4%
S3	$T_j^{sp} = 22°C$	Off	54.2	18.5%
S4	$T_j^{sp} = 22°C$	Off	59.5	17.6%
S5	$T_j^{sp} = 22°C$	Off	81.0	16.5%
S6	$PMV_j^{sp} = 0$	Off	69.0	6.4%

(-50%), respectively.

Taking a look at Tables 6 and 7, one can also note that due to the way the HVAC subsystems are managed using S3 (ESO) or S4 (ASOO), energy consumption is lower than it is when the predictive approach (S6) is considered. This is of course the consequence of a limited operation time, in particular for S4. With such a strategy, the subsystems operate up to 5 hours less a day (depending on the period of the year) than with S6. However, thermal comfort is much better with this last strategy. In heating mode (from November 1 to March 31, 2011), energy consumption is lower of about 21% with S3 and 13% with S4. Nevertheless, thermal comfort is degraded: 6.4% (S6) vs. 18.5% (S3) or 17.6% (S4). The same remarks apply

Table 7: Performance of the different strategies, $\forall j \in [\![1;3]\!]$. The simulation period is from June 1 to September 30, 2011 (cooling mode).

	Occupancy period	Non-occupancy period	Consumption (Wh/day m^2)	Discomfort criterion
S1	$T_j^{sp} = 22°C$	$T_j^{sp} = 22°C$	198.5	0.1%
S2	$T_j^{sp} = 22°C$	Off	122.6	0.2%
S3	$T_j^{sp} = 22°C$	Off	96.7	13.4%
S4	$T_j^{sp} = 22°C$	Off	90.5	25.4%
S5	$T_j^{sp} = 22°C$	Off	119.8	0.1%
S6	$PMV_j^{sp} = 0$	Off	116.2	0.1%

to the cooling mode (from June 1 to September 30, 2011). Energy consumption is lower with S3 (-16%) or S4 (-22%) but thermal comfort is clearly worse: 0.1% (S6) vs. 13.4% (S3) or 25.4% (S4).

5.2.2. Optimal switching times

Tables 8 and 9 give the optimal on/off switching times computed by the predicitive controller (S6) in heating and cooling modes, respectively, for two typical weeks. The simulation period is from January 6 to January 12, 2011 (heating mode) and from July 6 to July 12, 2011 (cooling mode). January 8-9 as well as July 9-10 are weekend days and the HVAC subsystems do not operate. Let us remember that R1 is for the ground floor offices, R2 is for the first floor offices and R3 is for the manufacturing area. One can highlight that the HVAC operation time is optimized (it is most of the time significantly reduced), whatever the room (comparison is between S2, the technique currently used in the real non-residential building, and S6). The daily time saved can reach up to 5 hours in January (heating mode) and about 2 hours in July (cooling mode). In addition, thermal comfort requirements are met.

5.2.3. Heating mode

Figs. 11 and 12 describe the way consumption of electrical power and thermal comfort evolve from January 6 to January 12, 2011 (heating mode) if the HVAC subsystems are managed using one of the basic techniques we described in section 5.1 (S1, S2, S3, S4 or S5) or the predictive approach we developed (S6). With S1 (Fig. 11(a)), overheating may happen during the afternoon and alters thermal comfort. Using the scheduling technique S2 (Fig. 11(b)), such an overheating is delayed or even avoided. As a result, thermal comfort is improved during the coldest periods. In addition, turning the HVAC subsystems off during non-occupancy periods allows energy consumption to be significantly reduced. Using S3 (Fig. 11(c)), the subsystems are turned on just when the employees start working in the non-residential building (i.e. at 8 a.m.). Consequently, thermal comfort constraints are not met for several hours in the morning. However, turning the HVAC subsystems off two hours before people leave in the late afternoon (i.e. at 4 p.m.) allows energy consumption to be reduced without any significant degradation of comfort, because of the thermal inertia of the considered non-residential building. As another scheduling technique, we considered S4 (Fig. 12(a)). Alternatively switching the HVAC subsystems on and off can be an interesting way of operating but only if thermal comfort has reached a sufficient level (for the considered non-residential building, after 11 a.m.). Earlier in the morning, energy storage is not enough and PMV_j, $\forall j \in [\![1;3]\!]$, can't be maintained in the desired interval (i.e. $[-0.5;+0.5]$). In addition, the PMV index exhibits high variability, what expresses the negative impact of such an HVAC operation mode on the thermal sensation of people. As an interesting point, one can observe in Fig. 12(a) that thermal comfort remains stable in the middle of the day in the first floor offices, because of the topology of the room (in particular, because of the presence of a large bay window). This is not the case in the two other rooms (the ground floor offices and the manufacturing area) where thermal comfort decreases faster. The last basic scheduling technique we considered is S5. As one can see in Fig. 12(b), pre-heating the rooms between 5 a.m. and 7 a.m. then turning the HVAC subsystems off during the hour preceding the arrival of the employees at the building (i.e. between 7 a.m. and 8 a.m.) do not lead to a satisfying thermal comfort at 8 a.m., especially in the ground floor offices. Indeed, during the hour the HVAC subsystems do not operate, the PMV index decreases quickly because of a low outdoor temperature and a limited sunshine, in spite of the building's thermal inertia. As a result, about 30 minutes are needed to reach an acceptable thermal comfort in this non-residential building. Between 12 p.m. and 1 p.m., stopping the subsystems does not produce the same effect and thermal comfort remains acceptable, because at that time of a higher outdoor temperature and a significant sunshine. Finally, with S6 (the predictive strategy), heating is stopped sooner than it is with the other techniques and overheating is completely avoided (Fig. 12(c)).

5.2.4. Cooling mode

Figs. 13 and 14 describe the way consumption of electrical power and thermal comfort evolve from July 6 to July 12, 2011 (cooling mode) if the HVAC subsystems are managed using one of the basic techniques we described in section 5.1 (S1, S2, S3, S4 or S5) or the predictive approach we developed (S6). With S1 (Fig. 13(a)), thermal comfort is perfect, whatever the hour of the day (and whatever the day of the week), but energy consumption is of course

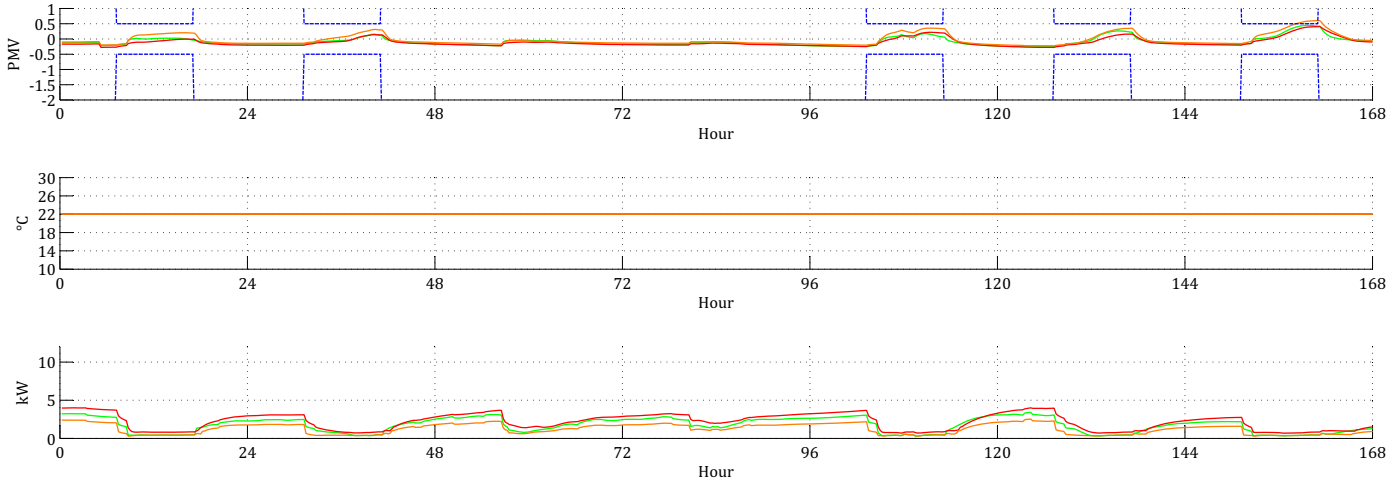

(a) Strategy S1. Energy consumption: 224.2 Wh/day m^2. Discomfort criterion: 1.8%.

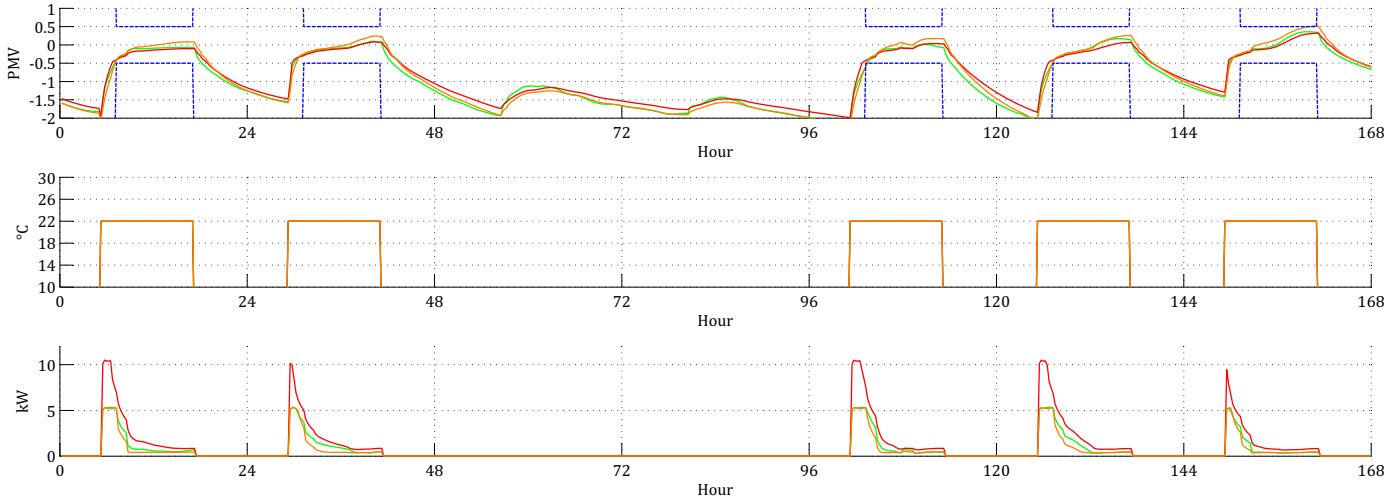

(b) Strategy S2. Energy consumption: 86.7 Wh/day m^2. Discomfort criterion: 1.0%.

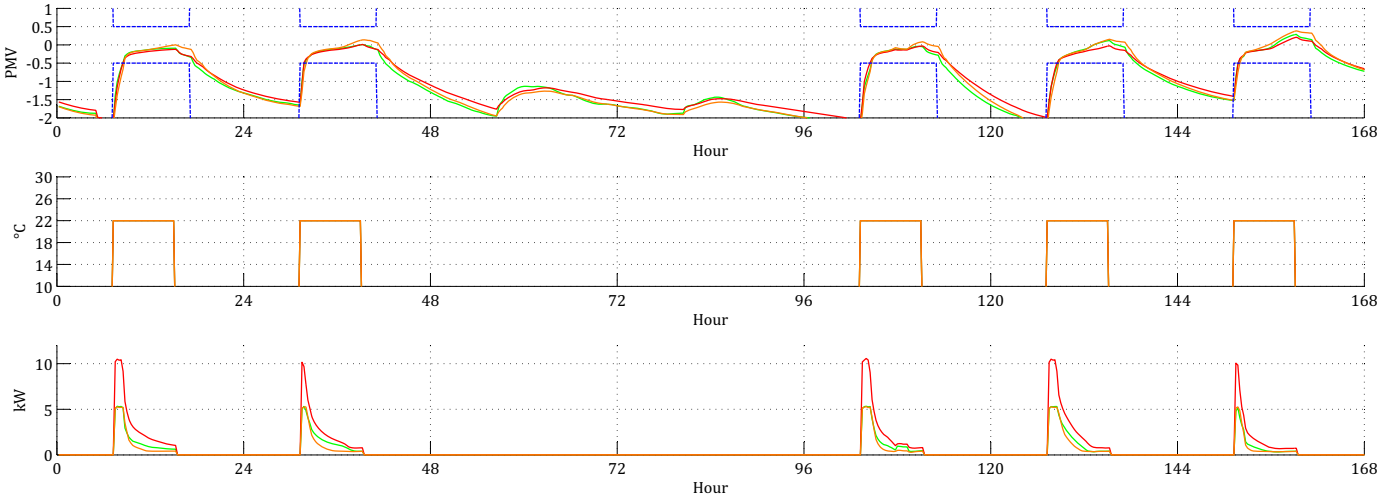

(c) Strategy S3. Energy consumption: 62.0 Wh/day m^2. Discomfort criterion: 15.3%.

Figure 11: Results from January 6 to January 12, 2011 (heating mode), using strategies S1 (a), S2 (b) and S3 (c). PMV_j (top), T_j^{sp} (middle) and P_j (bottom), $\forall j \in [\![1;3]\!]$. Green color is for the ground floor offices, orange color is for the first floor offices and red color is for the manufacturing area. Blue color is for PMV_j^{min} and PMV_j^{max}.

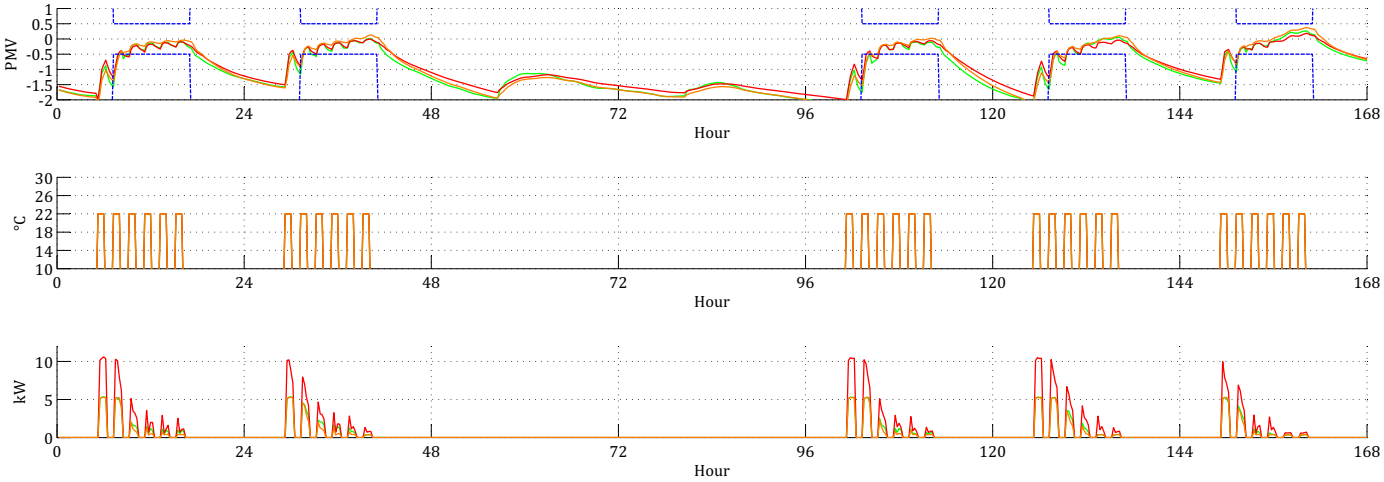

(a) Strategy S4. Energy consumption: 65.2 Wh/day m^2. Discomfort criterion: 14%.

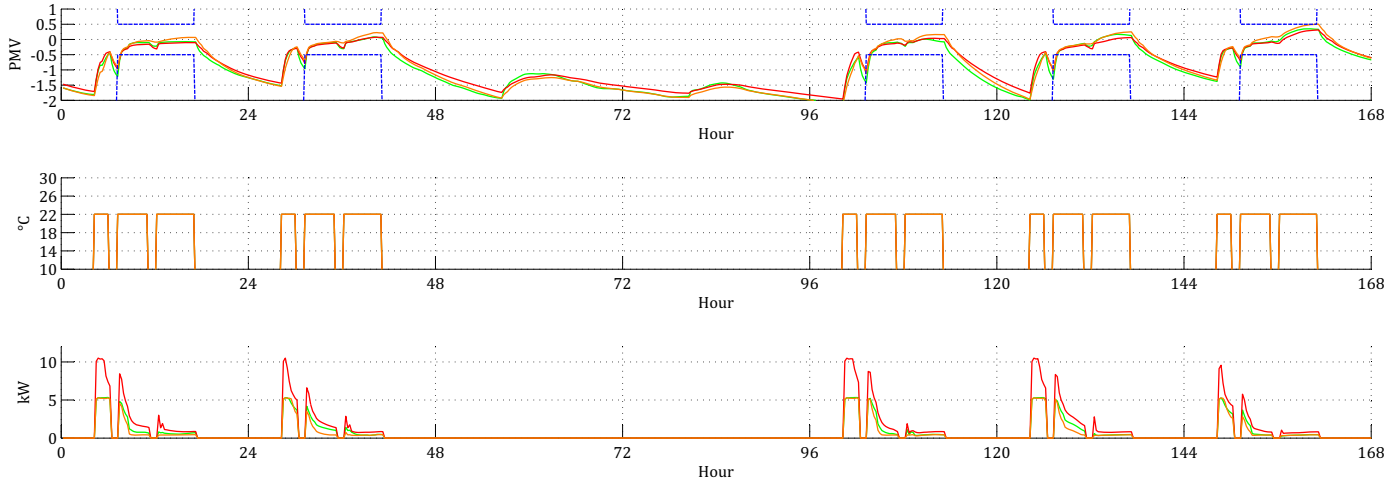

(b) Strategy S5. Energy consumption: 89.9 Wh/day m^2. Discomfort criterion: 4.3%.

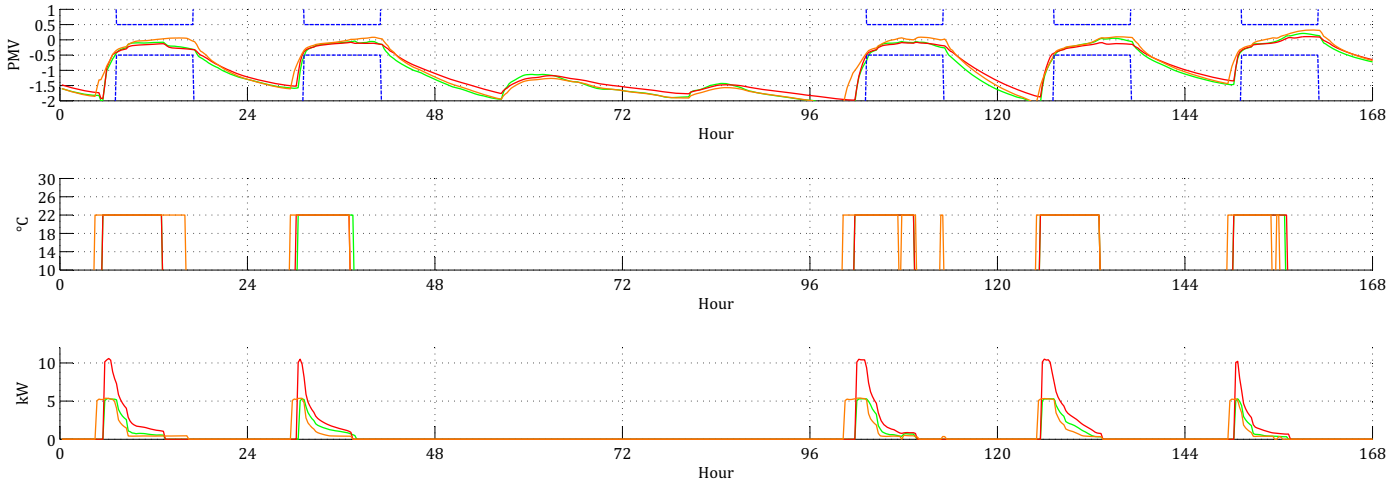

(c) Strategy S6. Energy consumption: 76.2 Wh/day m^2. Discomfort criterion: 0.7%.

Figure 12: Results from January 6 to January 12, 2011 (heating mode), using strategies S4 (a), S5 (b) and S6 (c). PMV_j (top), T_j^{sp} (middle) and P_j (bottom), $\forall j \in [\![1;3]\!]$. Green color is for the ground floor offices, orange color is for the first floor offices and red color is for the manufacturing area. Blue color is for PMV_j^{min} and PMV_j^{max}.

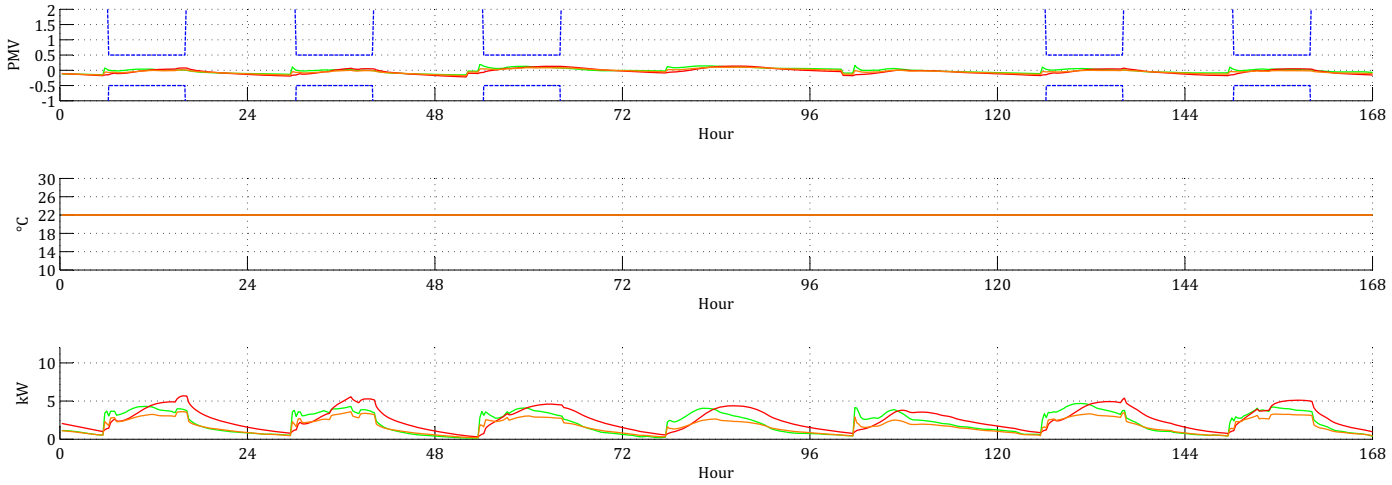

(a) Strategy S1. Energy consumption: 282.1 Wh/day m^2. Discomfort criterion: 0%.

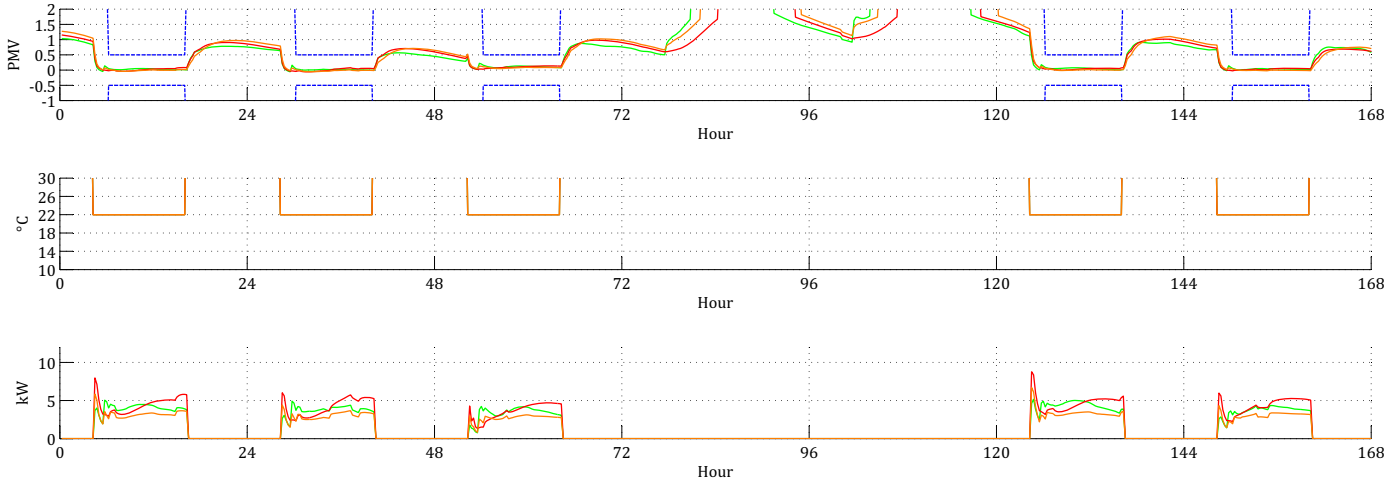

(b) Strategy S2. Energy consumption: 172.9 Wh/day m^2. Discomfort criterion: 0%.

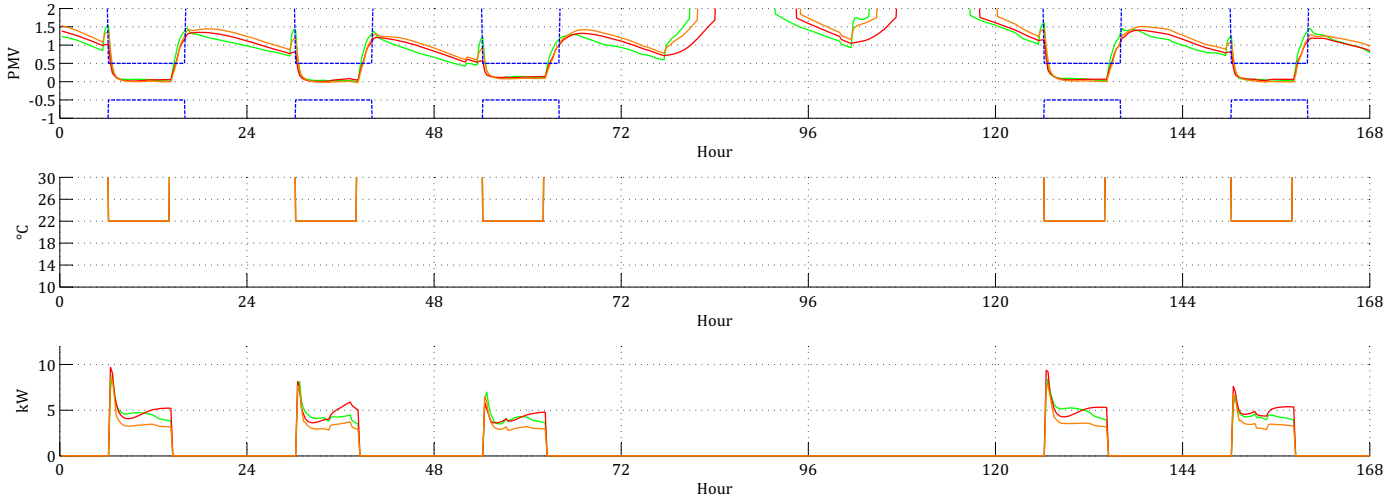

(c) Strategy S3. Energy consumption: 136.4 Wh/day m^2. Discomfort criterion: 18.3%.

Figure 13: Results from July 6 to July 12, 2011 (cooling mode), using strategies S1 (a), S2 (b) and S3 (c). PMV_j (top), T_j^{sp} (middle) and P_j (bottom), $\forall j \in [\![1;3]\!]$. Green color is for the ground floor offices, orange color is for the first floor offices and red color is for the manufacturing area. Blue color is for PMV_j^{min} and PMV_j^{max}.

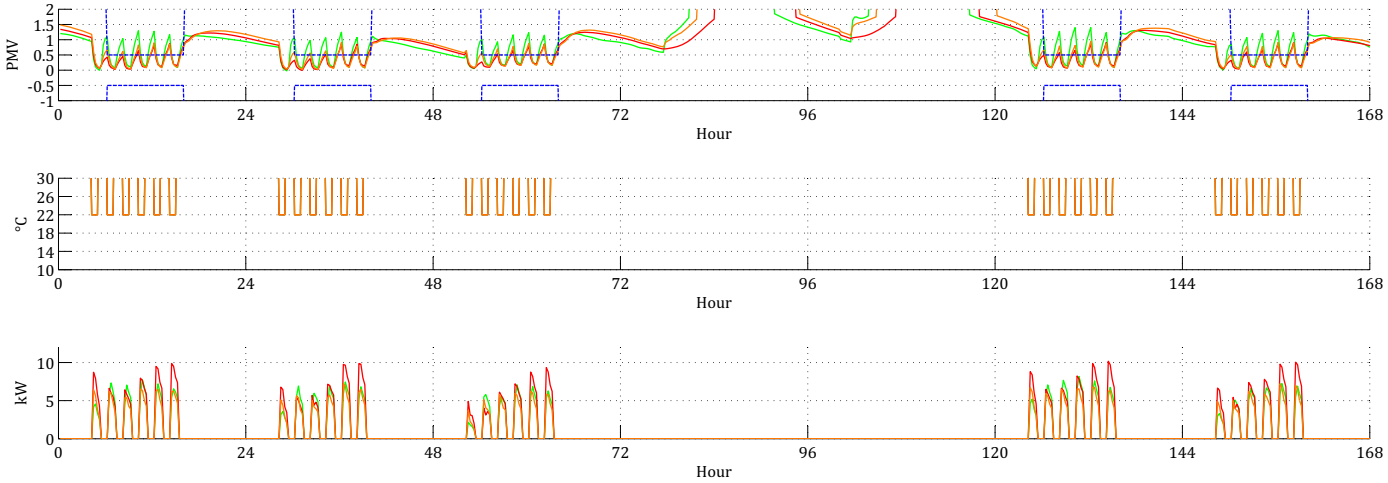

(a) Strategy S4. Energy consumption: 131.0 Wh/day m^2. Discomfort criterion: 34.3%.

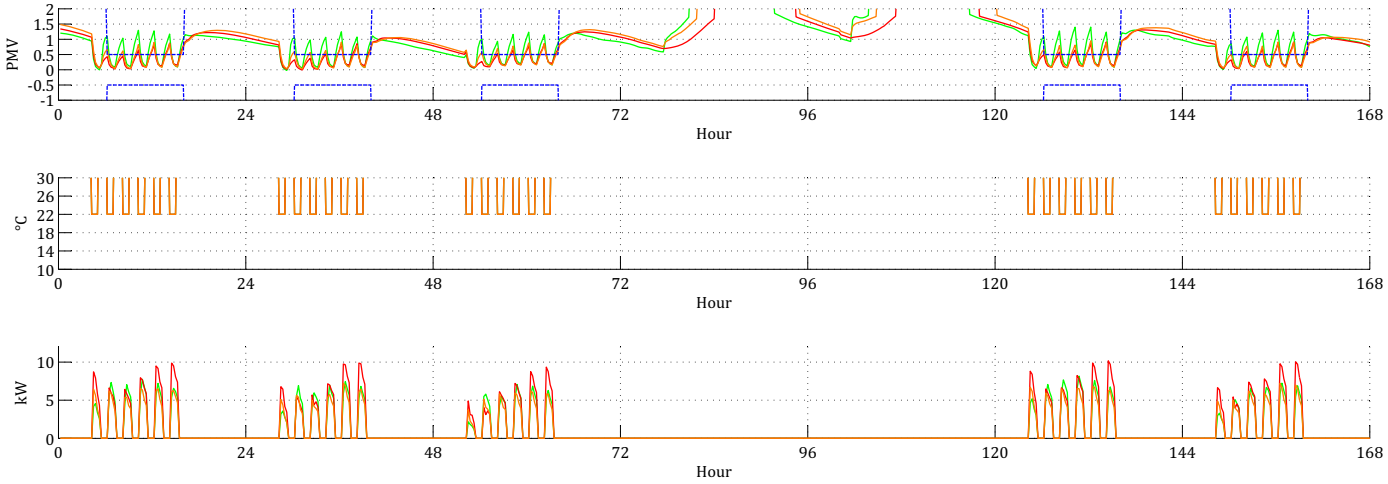

(b) Strategy S5. Energy consumption: 169.4 Wh/day m^2. Discomfort criterion: 6.8%.

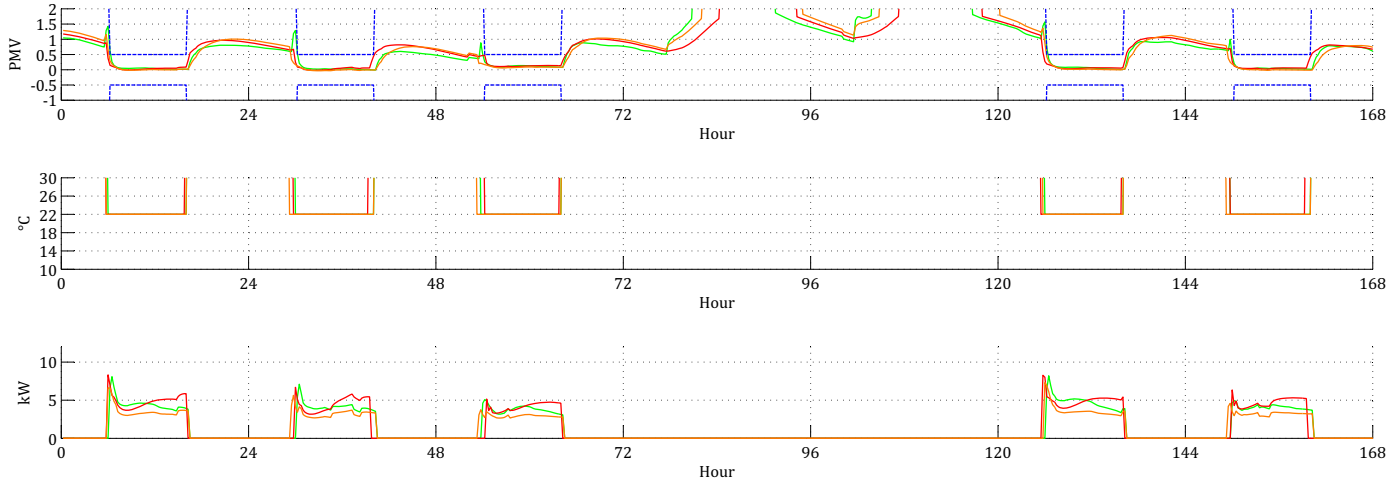

(c) Strategy S6. Energy consumption: 164.3 Wh/day m^2. Discomfort criterion: 0.5%.

Figure 14: Results from July 6 to July 12, 2011 (cooling mode), using strategies S4 (a), S5 (b) and S6 (c). PMV_j (top), T_j^{sp} (middle) and P_j (bottom), $\forall j \in [\![1;3]\!]$. Green color is for the ground floor offices, orange color is for the first floor offices and red color is for the manufacturing area. Blue color is for PMV_j^{min} and PMV_j^{max}.

Table 8: On/off switching times using S6. The simulation period is from January 6 to January 12, 2011 (heating mode). S2 is the reference.

	Day	Jan. 6	Jan. 7	Jan. 8	Jan. 9	Jan. 10	Jan. 11	Jan. 12
R1	Starting time	6:15 a.m.	7:15 a.m.	n/a	n/a	6:30 a.m.	6:15 a.m.	7:00 a.m.
	Stopping time	2:00 p.m.	2:30 p.m.	n/a	n/a	2:15 p.m.	2:00 p.m.	1:45 p.m.
	Time saved (h)	4:15	4:45	n/a	n/a	4:15	4:15	5:15
R2	Starting time	5:15 a.m.	6:15 a.m.	n/a	n/a	5:00 a.m.	5:45 a.m.	6:15 a.m.
	Stopping time	5:00 p.m.	2:00 p.m.	n/a	n/a	6:00 p.m.	2:00 p.m.	1:00 p.m.
	Time saved (h)	0:15	4:15	n/a	n/a	-1:00	3:45	5:15
R3	Starting time	6:15 a.m.	7:00 a.m.	n/a	n/a	6:30 a.m.	6:15 a.m.	7:00
	Stopping time	2:00 p.m.	2:00 p.m.	n/a	n/a	2:15 p.m.	2:00 p.m.	2:00 p.m.
	Time saved (h)	4:15	5:00	n/a	n/a	4:15	4:15	5:00

Table 9: On/off switching times using S6. The simulation period is from July 6 to July 12, 2011 (cooling mode). S2 is the reference.

	Day	July 6	July 7	July 8	July 9	July 10	July 11	July 12
R1	Starting time	7:45 a.m.	7:45 a.m.	7:30	n/a	n/a	7:45 a.m.	7:30 a.m.
	Stopping time	6:00 p.m.	6:00 p.m.	6:00 p.m.	n/a	n/a	6:00 p.m.	6:00 p.m.
	Time saved (h)	1:45	1:45	1:30	n/a	n/a	1:45	1:30
R2	Starting time	7:30 a.m.	7:00 a.m.	7:00 a.m.	n/a	n/a	7:30 a.m.	7:00 a.m.
	Stopping time	6:00 p.m.	6:00 p.m.	6:00 p.m.	n/a	n/a	6:00 p.m.	6:00 p.m.
	Time saved (h)	1:30	1:00	1:00	n/a	n/a	1:30	1:00
R3	Starting time	7:30 a.m.	7:30 a.m.	8:00 a.m.	n/a	n/a	7:15 a.m.	7:30
	Stopping time	5:45 p.m.	5:15 p.m.	5:45 p.m.	n/a	n/a	5:45 p.m.	5:15 p.m.
	Time saved (h)	1:45	2:15	2:15	n/a	n/a	1:30	2:15

very high (282.1 $\mathrm{Wh/day\,m^2}$). Using the scheduling technique S2 (Fig. 13(b)), comfort remains perfect whereas turning the HVAC systems off during non-occupancy periods allows energy consumption to be significantly reduced (172.9 $\mathrm{Wh/day\,m^2}$), in comparison to what is observed with S1. Using S3 (Fig. 13(c)), let us remember that the HVAC subsystems are turned on just when the employees start working in the building (i.e. at 8 a.m.). Thermal discomfort is observed for less than one hour during the morning (i.e. before 9 a.m.). However, turning the HVAC subsystems off two hours before people leave the building (i.e. at 4 p.m.) allows energy consumption to be reduced but thermal comfort is clearly degraded in the three considered rooms. This is the consequence of a low thermal inertia during summer. The next scheduling technique we considered is S4. Taking a look at Fig. 14(a), one can note that, similarly to what is observed in heating mode (i.e. from January 6 to January 12, 2011), PMV_j, $\forall j \in [\![1;3]\!]$, is hard to maintain in the desired interval (i.e. $[-0.5;+0.5]$) in the course of the morning. Thereafter, the increase in outdoor temperature allows thermal comfort to be acceptable. Clearly, both the low thermal inertia of the non-residential building as well as the temperatures observed in Perpignan (south of France) during summer impact negatively on the strategy's efficiency. S5 is the last basic scheduling technique we considered. As one can see in Fig. 14(b), pre-cooling the three considered rooms between 5 a.m. and 7 a.m. allows thermal comfort requirements to be met (barely) when the workers arrive at the building. As it has been stated previously, the first floor offices have a low thermal inertia and, as a result, the PMV index increases strongly (what leads to significant thermal discomfort) when the HVAC subsystem is turned off between 12 p.m. and 1 p.m. During this time, discomfort is weaker in the two other considered rooms of the building (the first floor offices and the manufacturing area). Finally, with S6 (the predictive strategy), cooling is stopped sooner than it is with the basic techniques (Fig. 14(c)). However, during hot periods, the benefits of using S6 are less important than in winter time. Indeed, in cooling mode, the HVAC subsystems cannot be turned off as soon as in heating mode. Anyway, using S6 to manage the HVAC subsystems of the non-residential building is clearly the best compromise between energy consumption and thermal comfort.

6. Conclusion

The present work deals with the predictive control of multizone Heating, Ventilation and Air-Conditioning (HVAC) systems in non-residential buildings. Such systems account for a large part of the energy consumption. Heating and cooling modes have been considered. In order to test the proposed approach, a real non-residential building located in Perpignan (south of France) has been modelled using the EnergyPlus software. We used the PMV

(Predicted Mean Vote) index as a thermal comfort indicator and developed low-order ANN-based models to be used as controller's internal models. The optimization problem has been solved using a genetic algorithm. The proposed strategy allows the operation time of each HVAC subsystem to be optimized (i.e. the right time to turn the HVAC subsystems on and off to be found) and thermal comfort requirements to be met. In comparison to what is observed when using a standard (non-predicitive) strategy, energy consumption is significantly reduced and thermal comfort is improved, whatever the operation mode and the period of the year. Future work will focus on implementing and validating the predictive strategy in the real building we modelled using the EnergyPlus software. Finally, natural ventilation will be considered in cooling mode with the aim of reducing energy consumption.

Acknowledgement

The authors want to thanks the Pyrescom company (`www.pyres.com`) for its financial support. Jean-Michel Cabanat and Cédric Calmon are acknowledged for their technical help and support.

References

[1] L. Pérez-Lombard, J. Ortiz, C. Pout, A review on buildings energy consumption information, Energy and Buildings 40 (3) (2008) 394–398.

[2] NF EN ISO 7730, Détermination analytique et interprétation du confort thermique par le calcul des indices PMV et PPD et par des critères de confort thermique local (2006).

[3] M. F. Haniff, H. Selamat, R. Yusof, S. Buyamin, F. S. Ismail, Review of hvac scheduling techniques for buildings towards energy-efficient and cost-effective operations, Renewable and Sustainable Energy Reviews 27 (2013) 94–103.

[4] G. Escriva, I. Segura-Heras, M. Alcazar-Ortega, Application of an energy and control system to assess the potential of different control strategies in hvac systems, Energy and Buildings 42 (11) (2010) 2258–2267.

[5] J. Murphy, N. Maldeis, Using time-of-day scheduling to save energy, ASHRAE Transactions 51 (5) (2009) 42–49.

[6] K. H. Lee, J. E. Braun, Development of methods for determining demand-limiting setpoints trajectories in buildings using short-term measurements, Buildings and Environment 43 (10) (2008) 1755–1768.

[7] K. H. Lee, J. E. Braun, Evaluation of methods for determining demand-limiting setpoints trajectories in buildings using short-term measurements, Buildings and Environment 43 (10) (2008) 1769–1783.

[8] T. Salsbury, P. Mhaskar, S. J. Qin, Predictive control methods to improve energy efficiency and reduce demand in buildings, Computers and Chemical Engineering 51 (2013) 77–85.

[9] J. E. Braun, Reducing energy costs and peak electrical demand through optimal control of building thermal storage, ASHRAE Transactions 96 (2) (1990) 876–887.

[10] P. Xu, P. Haves, Case study of demand shifting with thermal mass in two large commercial buildings, ASHRAE Transactions 115 (2) (2009) 586–598.

[11] S. S. Huang, Discriminatively trained patch-based model for occupant classification, Intelligent Transport Systems 6 (2) (2012) 132–138.

[12] M. M. Gouda, S. Danaher, C. P. Underwood, Thermal comfort based fuzzy logic controller, Building Services Engineering Research and Technology 22 (4) (2001) 237–253.

[13] A. Dounis, C. Caraiscos, Advanced control systems engineering for energy and comfort management in a building environment - A review, Renewable and Sustainable Energy Reviews 13 (6-7) (2009) 1246–1261.

[14] P. Bermejo, L. Redondo, L. de la Ossa, D. Rodríguez, J. Flores, C. Urea, J. A. Gámeza, J. M. Puerta, Design and simulation of a thermal comfort adaptive system based on fuzzy logic and on-line learning, Energy and Buildings 49 (2012) 367–379.

[15] M. Castilla, J. Álvarez, M. Berenguel, F. Rodríguez, J. Guzmán, M. Pérez, A comparison of thermal comfort predictive control strategies, Energy and Buildings 43 (10) (2011) 2737–2746.

[16] B. Paris, J. Eynard, S. Grieu, T. Talbert, M. Polit, Heating control schemes for energy management in buildings, Energy and Buildings 42 (10) (2010) 1908–1917.

[17] P.-D. Moroşan, R. Bourdais, D. Dumur, J. Buisson, Building temperature regulation using a distributed model predictive control, Energy and Buildings 42 (9) (2010) 1445–1452.

[18] A. Garnier, J. Eynard, M. Caussanel, S. Grieu, Low computational cost technique for predictive management of thermal comfort in non-residential buildings, Journal of Process Control 24 (6) (2014) 750 – 762.

[19] J. H. Holland, Adaptation in Natural and Artificial Systems, University of Michigan Press, Ann Arbor, Michigan, USA, 1975.

[20] S. Attia, M. Hamdy, W. O'Brien, S. Carlucci, Computational optimisation for zero energy buildings design: interviews results with twenty eight international expert, in: Proceedings of the 13th Internationcal Conference of the IBPSA, 2013, pp. 978–984.

[21] A. Kusiak, F. Tang, G. Xu, Multi-objective optimization of HVAC system with an evolutionary computation algorithm, Energy 36 (5) (2011) 2440–2449.

[22] T. Berthou, P. Stabat, R. Salvazet, D. Marchio, Optimal control for building heating: an elementary school case study, in: Proceedings of the 13th Internationcal Conference of the IBPSA, 2013, pp. 1944–1951.

[23] Y. Liu, Y. Pan, Z. Huang, Simulation-based receding-horizon supervisory control of HVAC system, in: Proceedings of the 13th Internationcal Conference of the IBPSA, 2013, pp. 1492–1498.

[24] P. O. Fanger, Assessment of man's thermal comfort in practice, British Journal of Industrial Medicine 30 (4) (1973) 313–324.

[25] S. Schiavon, K. H. Lee, Dynamic predictive clothing insulation models based on outdoor air and indoor operative temperatures, Building and Environment 59 (2013) 250–260.

[26] T. X. Nghiem, MLE+: a Matlab-EnergyPlus co-simulation interface (2010).

[27] S. Fahlman, The recurrent cascade-correlation architecture, R.P. Lippmann et al. (Eds), Advances in Neural Information Processing Systems, Morgan Kaufmann, Los Altos, USA, 1991.

[28] J. K. Spoerre, Application of the cascade correlation algorithm (cca) to bearing fault classification problems, Computers in Industry 32 (1997) 295 – 304.

[29] C. Charalambous, Conjugate gradient algorithm for efficient training of artificial neural networks, Circuits, Devices and Systems, IEE Proceedings G 139 (3) (1992) 301–310.

[30] D. S. Phatak, I. Koren, Connectivity and performance tradeoffs in the cascade-correlation learning architecture, IEEE Transactions on Neural Networks 5 (6) (1994) 930–935.

[31] M. Palonen, M. Hamdy, A. Hasan, Mobo a new software for multi-objective building performance optimization, in: Proceedings of the 13th Internationcal Conference of the IBPSA, 2013, pp. 2567–2574.

[32] T. Bäck, U. Hammel, H. Schwefel, Evolutionary computation: comments on the history and current state, IEEE Transactions on Evolutionary Computation 1 (1997) 3–17.

[33] L. M. Schmitt, Theory of genetic algorithms, Theoretical Computer Science 259 (1-2) (2001) 1–61.